J Appl Electrochem (2007) 37:505–510
DOI 10.1007/s10800-006-9282-0

ORIGINAL PAPER

Electrochemical characterization of the electrooxidation of methanol, ethanol and formic acid on Pt/C and PtRu/C electrodes

Zhaolin Liu · Liang Hong

Received: 22 August 2006 / Accepted: 28 November 2006 / Published online: 13 January 2007

Abstract Methanol, ethanol and formic acid electrooxidations in acid medium on Pt/C and PtRu/C catalysts were investigated. The catalysts were prepared by a microwave-assisted polyol process. Cyclic voltammetry and chronoamperometry were employed to provide quantitative and qualitative information on the kinetics of methanol, ethanol and formic acid oxidations. The PtRu/C catalyst showed higher anodic current densities than the Pt/C catalyst and the addition of Ru reduced the poisoning effect.

Keywords Pt nanoparticles · PtRu nanoparticles · Electrocatalysts · Methanol oxidation · Ethanol oxidation · Formic acid oxidation

1 Introduction

Methanol, ethanol and formic acid have all been considered as fuels in a direct liquid fuel cells. Methanol is considered the most appropriate fuel. On the other hand, ethanol electrooxidation was considered to be an important research topic as ethanol has much less toxicity and a higher specific energy. Methanol and ethanol 'crossover' from anode to cathode through the membrane lead to low system efficiency. Methanol and ethanol crossover limit utilization of high concentrations, generally less than 2 M. Feasibility of the PEM-based direct formic acid fuel cell (DFAFC) have been demonstrated by Masel et al. [1–3]. Hsing et al. [4] has also reported that the crossover can be reduced by five times and a higher performance can be achieved using formic acid when compared to methanol under the same conditions.

PtRu alloys are currently the most active anode catalyst for the oxidation of methanol or CO-contaminated H_2 (e.g. H_2 derived from reformed methanol) in low temperature solid polymer electrolyte fuel cells such as the direct methanol fuel cell (DMFC) [5–7] or the indirect methanol fuel cell (IMFC) [8]. In methanol reforming, methanol reacts with water to produce a reformate gas with a typical composition of 75% H_2, 24% CO_2 and about 1% CO. However, the performance of an IMFC is significantly affected by CO concentrations as low as a few ppm [9]. This is because of the strong adsorption of carbon monoxide on the Pt anode which inhibits the hydrogen oxidation reaction. PtRu alloys have similar H_2 oxidation kinetics as Pt electrocatalysts [10] but a much higher CO tolerance [11–14]. In the presence of Ru surface atoms, adsorbed CO is oxidized at potentials more negative than on Pt. Thus, the Pt surface sites become more available for hydrogen adsorption and oxidation. A carbon supported Pt catalyst for electro-oxidation of formic acid was founed to be poisoned severely by an adsorbed CO intermediate [15–17]. It was demonstrated that PtRu alloy was able to diminish this CO poisoning effect to some extent, but CO poisoning still significantly limited their catalytic activities for formic acid oxidation [18, 19].

Z. Liu (✉) · L. Hong
Institute of Materials Research & Engineering, 3 Research Link, Singapore 117602, Singapore
e-mail: zl-liu@imre.a-star.edu.sg

L. Hong
Department of Chemical and Biomolecular Engineering, National University of Singapore, 10 Kent Ridge Crescent, Singapore 119260, Singapore

In this work, the electrochemical properties of methanol, ethanol and formic acid oxidation on the Pt/C and PtRu/C electrodes were studied.

2 Experimental

The Pt/C and PtRu/C (20 wt.% Pt and 10 wt.% Ru on Cabot Vulcan XC-72) catalysts were prepared by microwave heating of ethylene glycol (EG) solutions of Pt or Pt and Ru salts. The atomic composition of the alloy was chosen to be close to Pt_{50}–Ru_{50}, the most active composition for the methanol electro-oxidation reaction [20]. A typical preparation would consist of the following steps: In a 100 ml beaker, 1.0 ml of an aqueous solution of 0.05 M $H_2PtCl_6 \cdot 6H_2O$ (Aldrich, A.C.S. Reagent) or 0.05 M $H_2PtCl_6 \cdot 6H_2O$ and 0.05 M $RuCl_3$ was mixed with 25 ml of ethylene glycol (Mallinckrodt, AR). About 0.5 ml of 0.4 M KOH was added dropwise. 0.040 g of Vulcan XC-72 carbon with a specific BET surface area of 250 $m^2\ g^{-1}$ and an average particle size of 40 nm was added to the mixture and sonicated. The beaker and its contents were heated in a household microwave oven (National NN-S327WF, 2450 MHz, 700W) for 50 s. The resulting suspension was filtered; and the residue was washed with acetone and dried at 373 K overnight in a vacuum oven.

The catalysts were examined by transmission electron microscopy (TEM) on a JEOL JEM 2010. A JEOL JSM-5600LV was used to determine the metal contents in the samples by energy-dispersive X-ray analysis (EDX). For microscopic examinations, the samples were first ultrasonicated in acetone for 1 h and then deposited on 3 mm Cu grids covered with a continuous carbon film. X-ray diffraction (XRD) patterns were recorded by a Bruker GADDS diffractometer with area detector using a Cu Kα source (λ = 0.1542 nm) operating at 40 kV and 40 mA.

An EG&G Model 263A potentiostat/galvanostat and a conventional three-electrode test cell were used for electrochemical measurements. The working electrode was a thin layer of Nafion-impregnated catalyst cast on a vitreous carbon disk held in a Teflon cylinder. The catalyst layer was obtained in the following way: (i) a slurry was first prepared by sonicating for 1 h a mixture of 0.5 ml of deionized water, 13 mg of Pt/C or PtRu/C catalyst, and 0.11 g of Nafion solution (Aldrich: 5 w/o Nafion); (ii) 2 µl of the slurry was pipetted and spread on the carbon disk; (iii) the electrode was then dried at 90 °C for 1 h and mounted on a stainless steel support. The surface area of the vitreous carbon disk was 0.125 cm^2 and the catalyst loading was therefore 0.3 mg cm^{-2} based on this geometric area. Pt gauze and a silver/silver chloride reference electrode (Ag/AgCl) were used as the counter and reference electrodes respectively**.** All potentials are quoted against Ag/AgCl electrode. All electrolyte solutions were deaerated by high-purity argon for 2 h prior to any measurement. For cyclic voltammetry and chronoamperometry of fuel oxidation, the electrolyte solution was 2 M methanol (or ethanol or formic acid) in 1 M H_2SO_4, which was prepared from high-purity sulfuric acid, high-purity grade methanol (or ethanol, or formic acid) and distilled water.

3 Results and discussion

In our approach, Pt and PtRu bimetallic nanoparticles are prepared and directly deposited on the carbon surface by microwave heating of ethylene glycol (EG) solutions of Pt and Ru salts. The supported bimetallic catalysts prepared as such are expected to maintain good electrocatalytic activity and CO tolerance in the direct alcohols and formic acid oxidations reaction at room temperature. The size and composition of the Pt and PtRu alloy particles were analyzed by TEM and point-resolved EDX measurements. Figure 1a and b are typical TEM images of Vulcan carbon-supported Pt and PtRu catalysts, showing a remarkably uniform and high dispersion of metal particles on the carbon surface. The particle size distributions of the metal in the supported catalysts were obtained by directly measuring the size of 100 randomly chosen particles in the magnified TEM images (Fig. 1c for Pt/C and Fig. 1d for PtRu/C sample). The average diameters of 4.3 ± 0.3 nm for Pt/C and 3.7 ± 0.3 nm for PtRu/C were accompanied by relatively narrow particle size distributions (2–6 nm). The microwave assisted heating of $H_2PtCl_6/RuCl_3/KOH/H_2O$ in ethylene glycol had evidently facilitated the formation of smaller and more uniform Pt and PtRu particles and their dispersion on Vulcan carbon support. It is generally agreed that the size of metal nanoparticles is determined by the rate of reduction of the metal precursor. The dielectric constant (41.4 at 298 K) and the dielectric loss of ethylene glycol are high, and hence rapid heating occurs easily under microwave irradiation. In ethylene glycol mediated reactions (the 'polyol' process), ethylene glycol also acts as a reducing agent to reduce the metal ion to metal powders. The fast heating by microwave accelerates the reduction of the metal precursor and the nucleation of the metal clusters. The easing of the nucleation limited process greatly assists in small particle formation. Additionally the homogeneous micro-

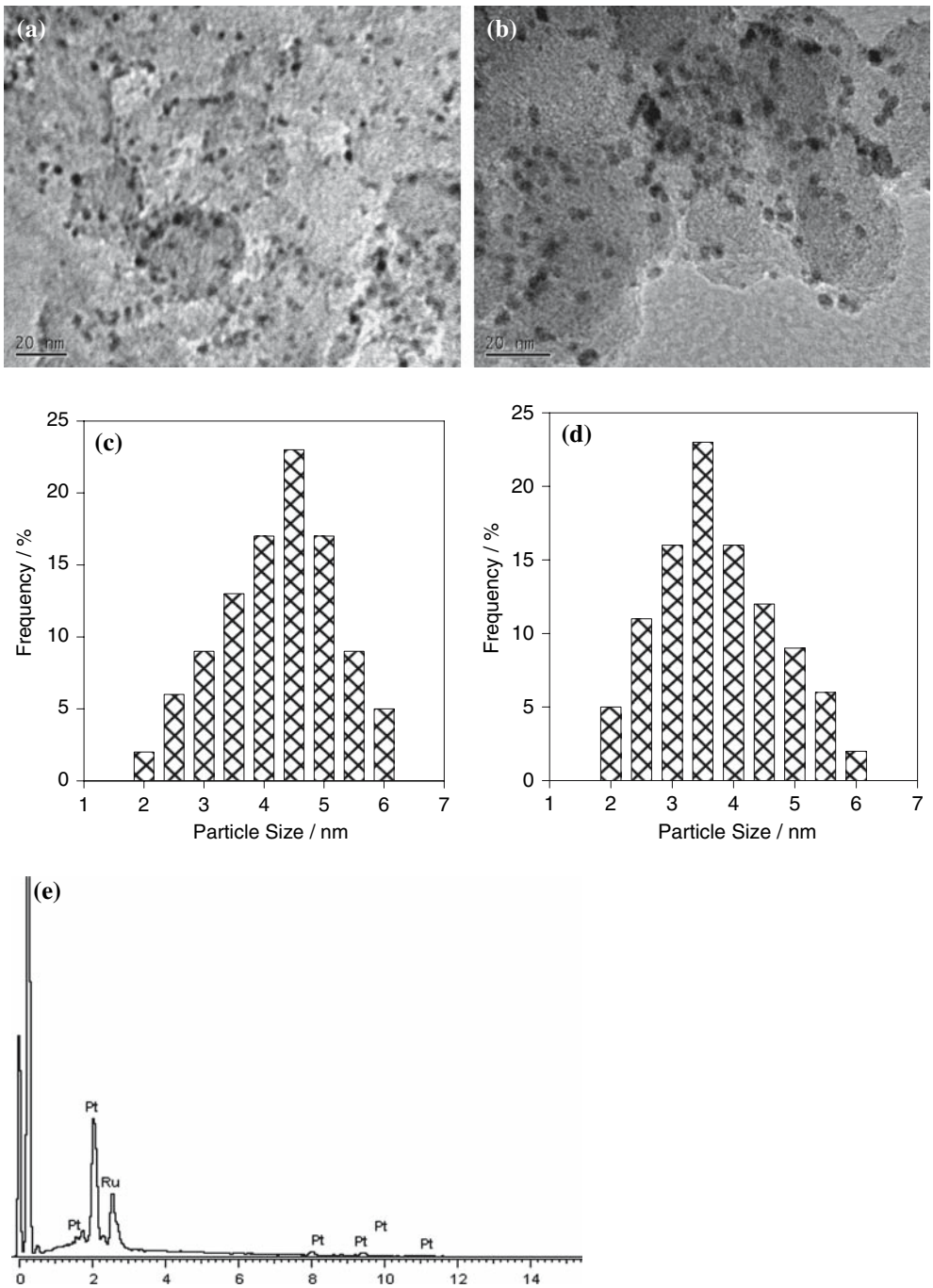

Fig. 1 TEM images of microwave-synthesized Pt/C (**a**) and PtRu/C (**b**) catalysts; Particle size distribution for Pt/C (**c**) and PtRu/C (**d**) catalysts; EDX spectra of PtRu/C catalyst (**e**)

wave heating of liquid samples reduces the temperature and concentration gradients in the reaction medium, thus providing a more uniform environment for the nucleation and growth of metal particles. The carbon surface may contain sites suitable for heterogeneous nucleation and the presence of a carbon surface interrupts particle growth. The smaller and nearly single dispersed Pt and PtRu nanoparticles on carbon XC-72 prepared by microwave irradiation can be rationalized in terms of these general principles. EDX measure (Fig. 1e) showed Pt content of 20.3 wt.% and Ru content of 9.8 wt.% for PtRu/C catalyst. The Pt/Ru atomic ratios was around 1.0:1.0–1.1, which agrees well with the stoichiometric ratio of 1:1 used for the preparation.

The powder X-ray diffraction (XRD) patterns for Pt/C and PtRu/C catalysts are shown in Fig. 2. PtRu/C catalyst displayed the characteristic patterns of Pt face-centered cubic (fcc) diffraction, except that the 2θ values were all shifted to slightly higher values. An

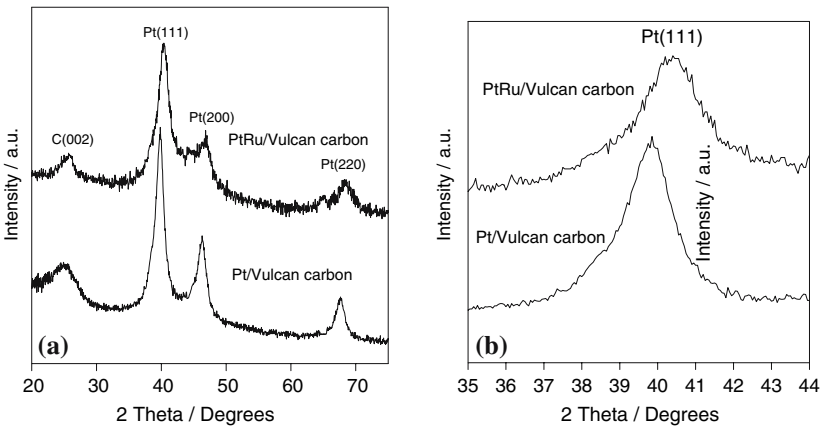

Fig. 2 (**a**) XRD pattern of microwave-synthesized Pt/C and PtRu/C catalysts; (**b**) an expanded view of the (111) reflections of the fcc phase

expanded view of the (111) reflections of the fcc phase is shown in Fig. 2b. The 2θ value of the (111) peak for PrRu/C was 40.5°, whereas the value was 39.9° for Pt/C. The same trend was replicated for the (200) and (220) diffraction.

Figure 3 shows cyclic voltammograms (CVs) of the methanol, ethanol and formic acid solutions for Pt/C catalyst. In the forward scan, methanol oxidation produced a prominent symmetric anodic peak around 0.75 V. In the reverse scan, an anodic peak current density was detected at around 0.50 V. Manohara and Goodenough [21] attributed this anodic peak in the reverse scan to the removal of the incompletely oxidized carbonaceous species formed in the forward scan. These carbonaceous species are mostly in the form of linearly bonded Pt–C ≡ O. Hence the ratio of the forward anodic peak current density (I_f) to the reverse anodic peak current density (I_b), I_f/I_b, can be used to describe the catalyst tolerance to carbonaceous species accumulation. Low I_f/I_b ratio indicates poor oxidation of methanol to carbon dioxide during the anodic scan, and excessive accumulation of carbonaceous residues on the catalyst surface. High I_f/I_b ratio shows the converse case. The forward scan oxidation peak of ethanol on Pt/C also appears at about 0.75 V. In the reverse scan, an anodic peak current density is detected at around 0.55 V. Iwasita and Pastor [22] reported that the adsorbed residues of ethanol (e.g. Pt–OCH_2CH_3, Pt–CHOH–CH_3, $(Pt)_2$ = COH–CH_3, Pt–$COCH_3$ and Pt–C ≡ O) are difficult to oxidize at low potentials. Thus, they constitute a catalyst poison. For the formic acid oxidation on Pt/C, the reaction commences in the hydrogen region and proceeds slowly in the forward scan direction reaching a plateau at 0.3 V. It corresponds to formic acid oxidation through dehydrogenation path but the coverage by CO_{ads} simultaneously continues to grow causing relatively small currents [23]. At potentials more positive than 0.65 V, the reaction becomes significantly accelerated and an anodic peak emerges at 0.75 V. This can be attributed to the oxidative removal of CO_{ads} and formic acid oxidation on sites that were previously blocked by CO_{ads}. At higher potentials formic acid oxidation is deactivated as a result of Pt surface oxidation. On the reverse scan, the surface stays inactive until partial reduction of the irreversibly formed surface oxides. One cathodic peak near 0.5 V is observed, which is due to the oxidation of formic acid after reduction of Pt oxides.

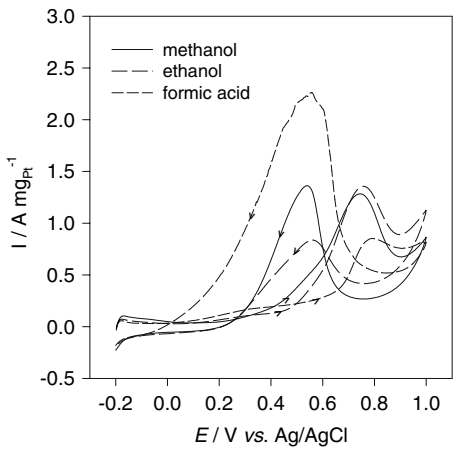

Fig. 3 Cyclic voltammograms of the Pt/C catalyst in 2 M methanol/1 M H_2SO_4, 2 M ethanol/1 M H_2SO_4 and 2 M formic acid/1 M H_2SO_4 with a scan rate of 50 mV s^{-1} at room temperature

Cyclic voltammograms for methanol, ethanol and formic acid oxidations on Pt/C catalyst in different the forward potential scan limit are shown in Fig. 4. Since the backward scan peak current decreases with increasing the anodic limit in the forward scan for methanol oxidation (Fig. 4a), it appears that the backward scan peak is primarily associated with

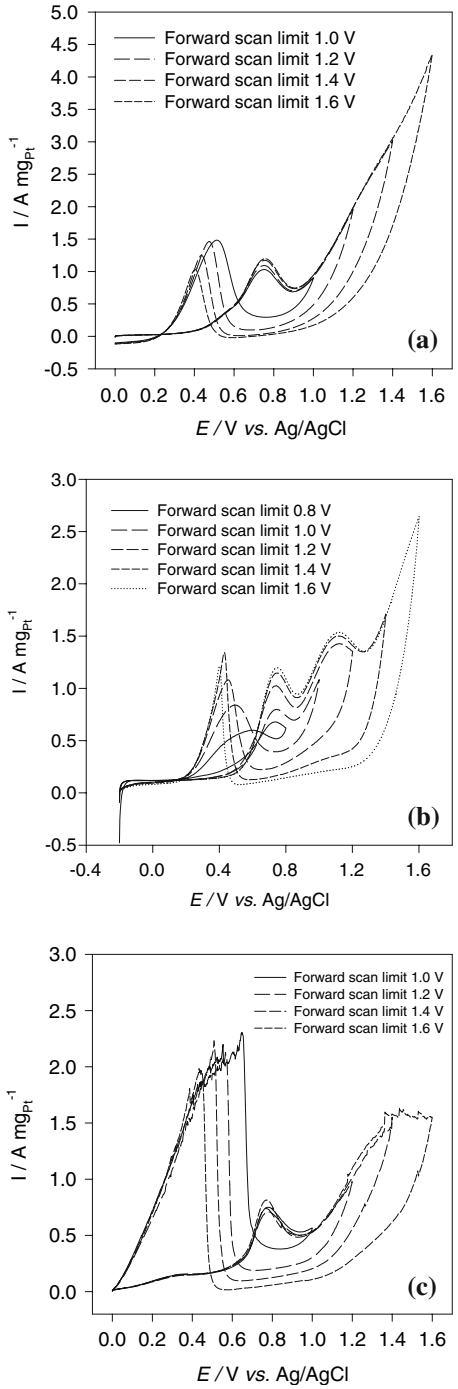

Fig. 4 Cyclic voltammograms of room temperature methanol, ethanol and formic acid oxidations on Pt/C catalyst in 2 M methanol/1 M H_2SO_4 (**a**), 2 M ethanol/1 M H_2SO_4 (**b**) and 2 M formic acid/1 M H_2SO_4 (**c**) at 50 mV s^{-1} in different the forward potential scan limit

residual carbon species on the surface rather than to the oxidation of freshly chemisorbed species. The reaction of the backward scan peak as mentioned by Manohara and Goodenough [21] would be written:

$$PtOH_{ad} + Pt - C \equiv O \rightarrow CO_2 + 2Pt + H^+ + e^-$$

Hence the I_f/I_b ratio increases with the anodic limit.

Since the backward scan peak current on Pt/C catalyst increases with increasing the anodic limit in the forward scan (Fig. 4b), it appears that the backward scan peak is associated with freshly chemisorbed species (such as CH_3–COOH and Pt–$(CO)_{ads}$). Since the backward scan peak current slightly decreases with increasing the anodic limit in the forward scan for the formic acid oxidation (Fig. 4c), it reveals that the backward scan peak is primarily associated with the oxidation of formic acid after reduction of Pt oxides.

Figure 5 shows cyclic voltammograms (CVs) of the methanol, ethanol and formic acid solutions for PtRu/C catalyst. There was no significant difference between the features of the voltammograms of PtRu/C and Pt/C catalysts. Anodic peaks appeared in both the forward and reverse (cathodic) scans. The peak current density around 0.75 V of methanol and ethanol oxidations on PtRu/C catalyst was somewhat higher than that on Pt/C catalyst. The PtRu/C catalyst had higher I_f/I_b ratio, consistent with the known high CO tolerance of PtRu catalysts. This can be attributed to the presence of Pt–Ru pair sites on the catalysts surface: Ru is known to adsorb oxygen-containing species (i.e., carbonaceous species) more favorably than pure Pt. For the PtRu/C catalyst, the formic acid oxidation shifts to lower potentials compared to the Pt/C catalyst. This shift indicates better electrocatalytic activity of the PtRu/C catalyst in the formic acid oxidation than Pt/C catalyst.

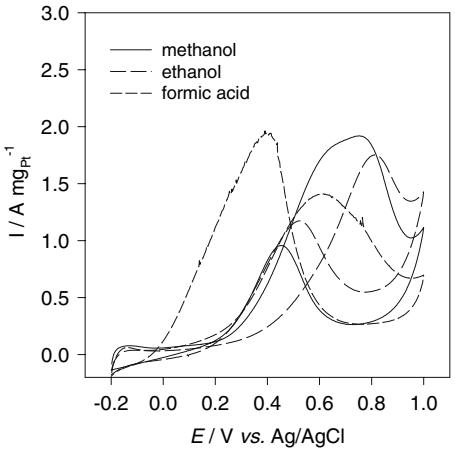

Fig. 5 Cyclic voltammograms of the PtRu/C catalyst in 2 M methanol/1 M H_2SO_4, 2 M ethanol/1 M H_2SO_4 and 2 M formic acid/1 M H_2SO_4 with a scan rate of 50 mV s^{-1} at room temperature

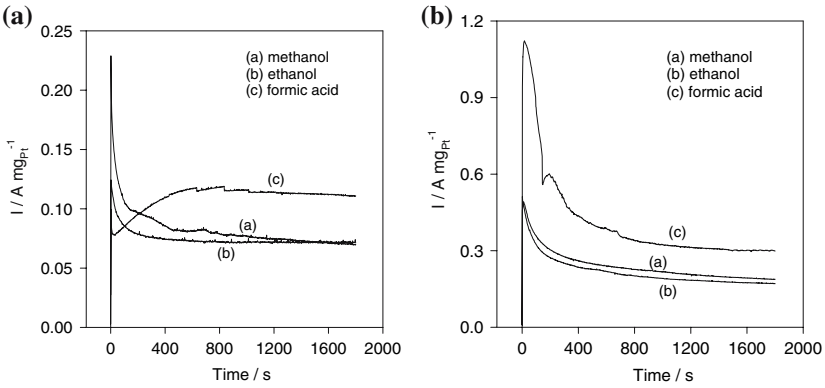

Fig. 6 Polarization current versus time plots for methanol, ethanol and formic acid oxidations on Pt/C (**a**) and PtRu/C (**b**) catalysts in 2 M methanol/1 M H_2SO_4, 2 M ethanol/1 M H_2SO_4 and 2 M formic acid/1 M H_2SO_4 at 0.4 V (versus Ag/AgCl) at room temperature

Pt/C and PtRu/C catalysts were biased at 0.4 V versus Ag/AgCl and the changes in their polarization currents with time were recorded (Fig. 6). As shown in Fig. 6a and b, the current density decayed with time and reached an apparent steady state within 600 s. Formic acid oxidation exhibits the highest current densities at the corresponding potential. The methanol oxidation shows slightly higher current density than that of ethanol oxidation. The results are in agreement with the cyclic voltammogram results. The PtRu/C catalyst had higher current density values at all corresponding potentials relative to the Pt/C catalyst.

4 Conclusions

Catalysts with smaller and nearly single dispersed Pt and PtRu nanoparticles on carbon XC-72 were prepared by a microwave-assisted polyol process. The current densities of methanol, ethanol and formic acid oxidations on PtRu/C catalyst were higher than that on Pt/C catalyst. The PtRu/C catalyst in methanol and ethanol solutions had higher peak current density in the forward scan and lower peak current density in the backward scan than the Pt/C catalyst, consistent with the known high CO tolerance of PtRu catalyst. For the PtRu/C catalyst, the formic acid oxidation shifts to lower potential values compared to the Pt/C catalyst. This shift indicates better electrocatalytic activity of the PtRu/C catalyst for formic acid oxidation than Pt/C catalyst. Chronoamperometry data show that formic acid oxidation on both the Pt/C and PtRu/C catalysts is more active than for that of methanol and ethanol.

References

1. Rice C, Ha S, Masel RI, Waszczuk P, Wieckowski A, Barnard T (2002) J Power Sources 111:83
2. Rice C, Ha S, Masel RI, Wieckowski A (2003) J Power Sources 115:229
3. Zhu Y, Ha S, Masel RI (2004) J Power Sources 130:8
4. Wang X, Hu JM, Hsing IM (2004) J Electroanal Chem 562:73
5. Cameron CS, Hards GA, Thompsett D (1992) Direct methanol-air fuel cells, The Electrochemical Society Proceedings Series, Pennington NJ PV 92–14, p 10
6. Ren X, Wilson MS, Gottesfeld S (1996) J Electrochem Soc 143:L12
7. Wasmus S, Vielstich W (1993) J Appl Electrochem 23:120
8. Oetjen HF, Schmidt VM, Stimming U, Trila F (1996) J Electrochem Soc 143:3838
9. Lemons RA (1990) J Power Sources 29:251
10. Gasteiger HA, Markovic N, Ross PN (1995) J Phys Chem 99:8290
11. Gasteiger HA, Markovic N, Ross PN, Cairns EJ (1994) J Phys Chem 98:617
12. Liu ZL, Lee JY, Chen WX, Han M, Gan LM (2004) Langmuir 20:181
13. Liu ZL, Ling XY, Su XD, Lee JY (2004) J Phys Chem B 108:8234
14. Liu ZL, Ling XY, Su XD, Lee JY, Gan LM (2005) J Power Sources 149:1
15. Jiang J, Kucernak A (2002) J Electroanal Chem 520:64
16. Park S, Xie Y, Weaver MJ (2002) Langmuir 18:5792
17. Lovic JD, Tripkovic AV, Gojkovic SL, Popovic KD, Tripkovic DV, Olszewski P, Kowal A (2005) J Electroanal Chem 581:294
18. Capon D, Parsons R (1975) J Electroanal Chem 65:285
19. Arenz M, Stamenkovic V, Schmidt TJ, Wandelt K, Ross PN, Markovic NM (2003) Phys Chem Chem Phys 5:4242
20. Takasu Y, Fujiwara T, Murakami Y, Sasaki K, Oguri M, Asaki T, Sugimoto W (2000) J Electrochem Soc 147:4421
21. Manohara R, Goodenough JB (1992) J Mater Chem 2:875
22. Iwasita T, Pastor E (1994) Electrochimica Acta 39:531
23. Jovanovic VM, Tripkovic D, Tripkovic A, Kowal A, Stoch J (2005) Electrochem Commun 7:1039